Available online at www.sciencedirect.com
SCIENCE DIRECT
Geomorphology 71 (2005) 139–155
GEOMORPHOLOGY
www.elsevier.com/locate/geomorph

Statistical analysis of lateral migration of the Rio Grande, New Mexico

Gigi A. Richard[a,*], Pierre Y. Julien[b], Drew C. Baird[c]

[a]Department of Physical and Environmental Sciences, Mesa State College, Grand Junction, CO 81501, USA
[b]Engineering Research Center, Colorado State University, Fort Collins, CO 80523, USA
[c]U.S. Bureau of Reclamation, Albuquerque, NM 87102, USA

Received 15 December 2002; received in revised form 30 June 2004; accepted 1 July 2004
Available online 19 April 2005

Abstract

The lateral migration rates of alluvial rivers are affected by changes in water and sediment regimes. The Rio Grande downstream from Cochiti Dam exhibits spatial and temporal variability in lateral movement rates documented since 1918. A tremendous database exists that documents planform, bed material size, channel geometry, and water and sediment regimes. A statistical analysis reveals that migration rates primarily decreased with decreasing flow energy ($R^2>0.50$, $p<0.0001$). The addition of a second parameter describing total channel width increased the explained variance to >60%. The findings show that lateral movement increases with increasing flow energy and with degree of braiding.

Keywords: Channel adjustment; Dams; Rio Grande; Channel stability; Stream power

1. Introduction

The successful and sustainable management of a river corridor requires an understanding of which reaches are more susceptible to lateral migration. Lateral adjustments result from changes in hydraulic, sediment, and channel bank characteristics. High lateral migration rates result in property loss and can threaten urban populations through increased risks of flooding. On the other hand, reduced lateral migration rates can translate into declining habitat quality. Habitat restoration efforts often require a laterally mobile channel whereas engineering management often attempts to reduce risk to riverside structures and communities through a laterally stable channel. Lateral migration rates can vary both spatially and temporally within a single river reach (e.g., Hooke, 1980; Lawler et al., 1999). Anthropogenic impacts such as dam construction can affect migration rates as well (e.g., Xu, 1996, 1997; Shields et al., 2000).

* Corresponding author. Tel.: +1 970 248 2689; fax: +1 970 248 2700.
E-mail addresses: grichard@mesastate.edu (G.A. Richard), pierre@engr.colostate.edu (P.Y. Julien).

0169-555X/$ - see front matter © 2005 Elsevier B.V. All rights reserved.
doi:10.1016/j.geomorph.2004.07.013

1.1. Lateral movements

Several studies used statistical analyses to define relationships between measured lateral movement rates and hydraulic, sediment, and other channel-form variables (Table 1). The important variables in describing and predicting lateral movement rates are channel form, sinuosity and curvature of bends, stream power, stream size measured by width or drainage area, sediment supply, and bank material, stability, and vegetation. The studies summarized in Table 1 suggest that the spatial and temporal variability of lateral migration are associated with variability in flow energy, bed material size, suspended sediment discharge, river size (channel width), and planform geometry.

Table 1
Summary of published relationships between lateral migration rates and other parameters

Source	Significant relationship	Notes
Hooke (1979)	$M \sim Q_{peak}$, API	API=Antecedent precipitation index
Hooke (1980)	$M \sim A$ (drainage area) $M \sim$% silt-clay in bank	
Hickin and Nanson (1975), Nanson and Hickin (1983)	$M \sim R_c/W$	Also identified bank texture, planform, and sediment supply rate as important
Begin (1981)	$M \sim R_c/W$	
Nanson and Hickin (1983)	$M \sim Q$ and S $M \sim W$ and S $M \sim Q$, S and D_{50} $M \sim W$, S and D_{50}	
Hickin and Nanson (1984)	$M \sim R_c/W$	Also identified bank resistance as important
Biedenharn et al. (1989)	$M \sim R_c/W$	
Thorne (1991)	$M \sim R_c/W$	Also identified bank material and geologic controls as important
Klaassen and Masselink (1992)	$M \sim W$, R_c/W	Assuming that bank resistance and sediment concentration do not vary. Bank vegetation was not important
MacDonald (1991)	$M \sim h$ $M \sim Q$	
Lawler et al. (1999)	$M \sim L$	L=distance downstream. Also found stream power and bank material to be important
Shields et al. (2000)	$M \sim W$, R_c/W	Comparing pre- and post-dam rates

Lateral migration rates often increase with flow energy, which includes the kinetic energy of the water discharge and the potential energy measured by either the valley or channel slope. Hooke (1979), Nanson and Hickin (1986), MacDonald (1991), and Lawler et al. (1999) found that lateral migration rates increase with flow energy in meandering rivers. Bledsoe and Watson (2001) found that measures of stream power were significantly correlated with the degree of lateral stability in river channels measured by the transition to braiding. Along those same lines, Knighton and Nanson (1993) proposed that high flow energy was necessary for planform shifts from meandering to braided. However, Brice (1982) showed that both braided and meandering streams exhibited either high or low lateral mobility, depending on other factors. He suggested that the lateral mobility of meandering rivers is a function of downstream variability in width. For braided rivers, if the braidplain is sinuous and point bars are visible, the rivers tend to be highly mobile; but if a braided river is straight and wide, it tends to be more stable. These wide, straight, braided rivers are typically adjusted to a very large discharge, i.e., flow energy.

The planform geometry of channels also relates to lateral migration rates. Several studies found that there is a maximum erosion rate for meandering rivers corresponding to an R_c/W somewhere between two and three (Hickin and Nanson, 1975, 1984; Nanson and Hickin, 1983; Biedenharn et al., 1989). The correlation between radius of curvature and migration rate suggests that there is also a value for sinuosity that would correlate to maximum lateral migration rates. The channel width has been noted to be important in association with lateral migration (Brice, 1982; Nanson and Hickin, 1986). Channel width has also been used to scale for flow energy and for river size (Brice, 1982; Nanson and Hickin, 1986) and as such could be a useful variable for correlation with lateral movement.

The relationship between bed material size and migration rate varies. A fine bed material (non-cohesive) is easier to transport and erode. As Nanson and Hickin (1986) showed, the bed material size at the

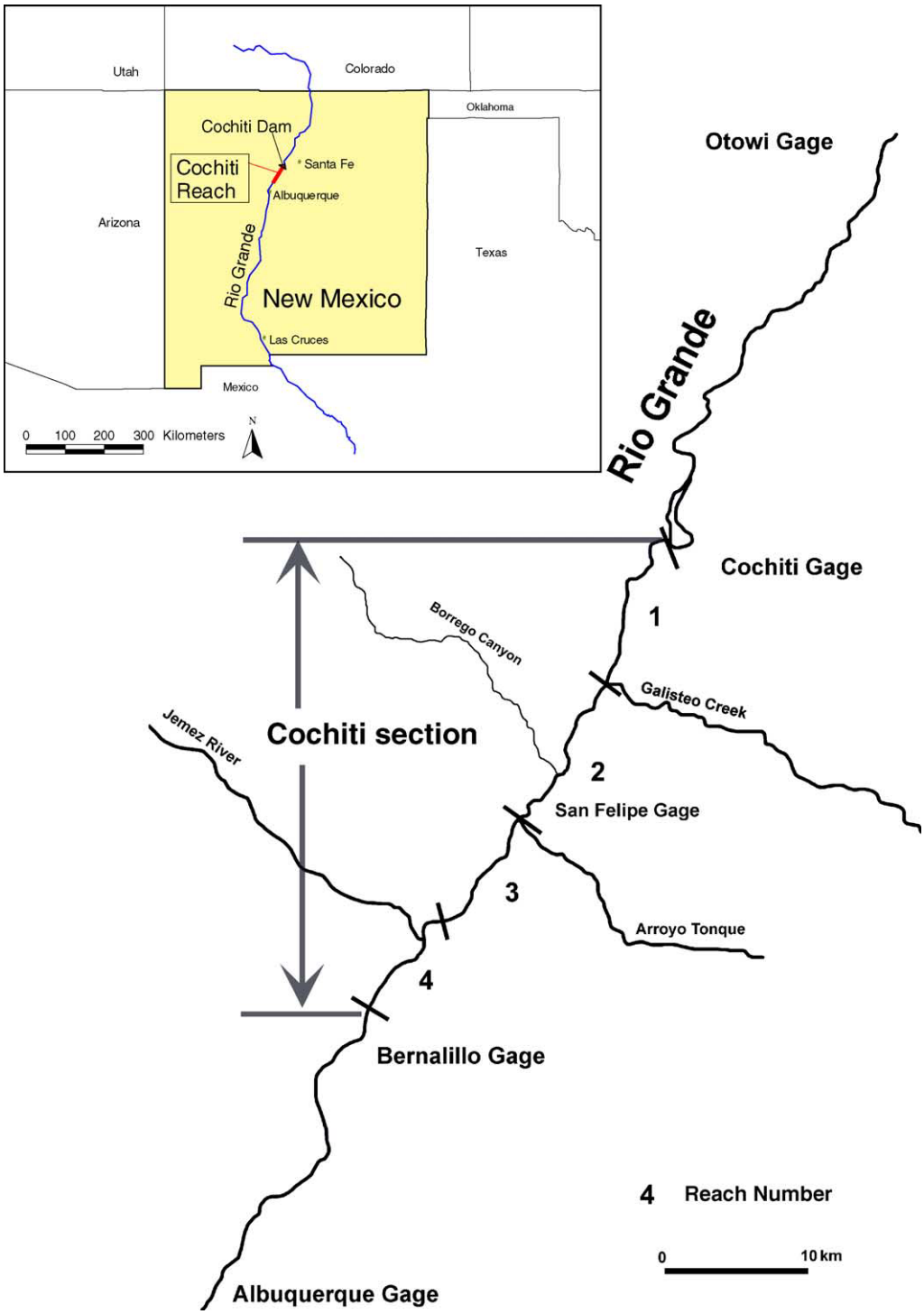

Fig. 1. Cochiti section, Rio Grande, New Mexico.

toe of the slope can be a good indication of the resistance of the bank. At the other extreme, for instance downstream from a dam, armored beds are no longer mobile and the flow often scours the banks. Additionally, incision associated with armoring results in high, often unstable banks. The result is that high lateral migration rates can be associated with both small and large bed material size. However, it would be expected that the highest rates would be associated with smaller sized material in a wandering/braided river.

Sediment supply also impacts the rate of lateral migration. Carson (1984) suggested that a high sediment supply is an important factor for the development of braiding and that the banks are often a source of sediment. High rates of sediment transport can result in aggradation and avulsion, whereas extremely low sediment supply encourages bed and bank erosion. Bledsoe (1999) suggests that sediment supply and bank resistance determine whether instability in a channel is manifested laterally (braiding) or vertically (incision). The sediment transport balance between the transport capacity of the channel and the sediment supply from upstream sources is also very important. Channels will aggrade and possibly avulse when sediment transport is capacity limited (i.e., the supply exceeds the transport rate). On the other hand, channel incision and potential bank erosion result when the reach is supply limited. The state of equilibrium occurs when the sediment transport capacity of a reach equals the sediment supply (Julien, 2002).

1.2. Objectives

This study provides a statistical analysis of the parameters affecting the lateral movement of the Rio Grande in New Mexico. The first objective of this paper is to determine significant relationships between lateral migration rates and changes in flow energy, sediment supply, bed material, and planform geometry between pre and post-dam conditions of the Rio Grande. The second objective is to model changes in lateral migration of the channel using a statistical analysis. The final objective is to determine the predictive capabilities of the resulting models. The models were calibrated using the 1918 to 1992 database of the Rio Grande below Cochiti Dam and validated using the 1992–2001 data. Richard (2001) provided the background information required to undertake this analysis.

2. Study site

The Cochiti section extends about 45 km downstream from Cochiti Dam (Fig. 1), which was completed in November 1973 for the purposes of flood control and sediment detention (U.S. Army Corps of Engineers, 1978). Cochiti Reservoir provides the largest flood control storage volume (500,000 ac-ft) on the main stem of the Rio Grande. With an entire drainage area of about 37,800 km^2 (Bullard and Lane, 1993), the dam traps virtually the entire sediment load from upstream as well as controlling the water discharge (Dewey et al., 1979; Richard, 2001).

Construction of the dam has resulted in significant impacts on the channel downstream (Lagasse, 1980, 1981, 1994; Leon, 1998; Bauer, 1999; Richard, 2001; Richard and Julien, 2003; Schmidt et al., 2003). Prior to construction of Cochiti Dam, the average active channel width was about 275 m; and the Cochiti section exhibited characteristics of braiding with up to four channels at some cross-sections (Lagasse, 1980; Richard, 2001). Since construction of Cochiti Dam, the active channel width averages about 90 m and a majority of the river flows in a single thread channel (Richard and Julien, 2003). Degradation following closure of the dam has been documented as far as 200 km downstream from the dam (Sanchez and Baird, 1997). The bed of the river in the first few miles downstream of the dam has armored to a gravel/cobble bed (Leon, 1998). Bed degradation and lateral migration still occur in some portions of the river, but the general trend of the reach appears to be toward a more stable state (Richard, 2001).

3. Methods

3.1. Database

The combination of severe flooding, sedimentation, and irrigation needs in the middle Rio Grande valley in the early 1900s prompted state and federal agencies [including the U.S. Army Corps of Engineers

(the Corps), the U.S. Bureau of Reclamation (USBR), the U.S. Geological Survey (USGS) and the Soil Conservation Service (SCS, now the Natural Resources Conservation Service, or NRCS)] to begin intensive surveys of the river. Data collection had begun on the Rio Grande in 1889 with the establishment of the first gaging station in the United States at Embudo, NM by the USGS. In 1895, the Otowi station (Fig. 1) was established and provides the longest record of discharge and suspended sediment data used in this study. Cross-section surveys were collected beginning in 1918, bed material sampling began in the 1930s, suspended sediment measurements were initiated in the 1940s, and aerial photography or topographic surveys are available from 1918 to 1992. The net result of these data collection efforts is a comprehensive documentation of the Cochiti section for almost 100 years.

Numerous data sources were combined to complete this study. The data sources are thoroughly documented in Richard (2001) and Richard and Julien (2003). The sources include a database of cross-section, sediment, and discharge data compiled by Leon (1998) and Leon et al. (1999). In addition, the lateral movement, width, and planform data were obtained from a series of aerial photos and topographic surveys (1918, 1935, 1949, 1962, 1972, 1985, 1992, and 2001). The USBR Remote Sensing and GIS group digitized the non-vegetated active channel from the aerial photos (USBR, 1998). During the winter of 2000/2001, the USBR took another set of aerial photos of the Rio Grande. Inclusion of the 2001 photos extends this study beyond Richard (2001). The Cochiti section was divided into four smaller study reaches and 26 subreaches based on channel characteristics and the existence of natural or manmade controls (Fig. 1 and Table 2).

Table 2
Reach definition and lengths

Reach no.	Description	Valley length (km)	Average Thalweg length (km)
1	Cochiti Dam-Galisteo Creek	11.9	13.2
2	Galisteo Creek-Arroyo Tonque (San Felipe)	11.3	13.1
3	Arroyo Tonque-Angostura Diversion Dam	9.4	9.9
4	Angostura Diversion Dam-Bernalillo (Hwy 44 Bridge)	9.7	10.6

3.2. Measurement of independent and dependent variables

The database was subdivided into seven study periods (1918–1935, 1935–1949, 1949–1962, 1962–1972, 1972–1985, 1985–1992, 1992–2001), four reaches, and 26 subreaches. Measurements of lateral migration, flow energy, sediment supply, channel width, and channel planform of each reach and subreach were compiled for each study period and each of the reaches and subreaches.

3.2.1. Lateral migration

Lateral migration rates of the Cochiti section were estimated by measuring the displacement of the outermost banklines. Displacements of each the right and left banks were measured using the GIS coverages of the active channel at each of 284 cross-sections located ~150 m apart. Changes in total width of the channel were subtracted from the displacement so that the resulting movement rate represents migration and not width change of the channels. The cross-section values were then averaged over the four reaches and 26 subreaches. An average annual lateral migration rate for each time period was computed by dividing the lateral migration for the time period by the length of the time period (Richard, 2001).

3.2.2. Flow energy

The flow energy combines the effects of discharge, Q, and slope, S. The peak mean-daily discharge, Q, for the time period between aerial surveys is used as the representative discharge value for each time period (Richard, 2001). For example, for the 1918 and 1935 surveys, the representative discharge is the peak mean daily discharge between 1918 and 1934. Reach-averaged slope values, S, are computed from cross-section survey and profile data (Richard, 2001). The value of the slope at the beginning (or the closest to the beginning) of each time period is used.

The total and specific stream power are important indicators of the erosive power and energy of flow in stream channels. Nanson and Hickin (1983) proposed

that total stream power, $\Omega=\gamma QS$, where γ is the specific weight of water, Q is discharge and S is slope, could be a factor in influencing lateral migration rates. Specific stream power,

$$\omega = \frac{\gamma QS}{W}, \quad (1)$$

where W=channel width, has also been associated with changes in channel planform (Carson, 1984; Ferguson, 1987; Nanson and Croke, 1992) and lateral migration (Nanson and Hickin, 1986). Substituting the relationship between channel width and the square root of dominant discharge (Ferguson, 1987; Knighton, 1998), $W=\alpha Q^{0.5}$, into the definition of specific stream power yields an approximation of specific stream power of the form (Bledsoe, 1999):

$$\frac{\gamma}{\alpha}\sqrt{Q}\cdot S \quad (2)$$

where α is an empirically derived constant.

Surrogates for both total and unit stream power are used in the model in the forms of QS and $S\sqrt{Q}$, respectively, where Q is the peak discharge for the time period and S is the channel slope estimated for each reach. The specific weight of water is omitted because of its relative constancy in natural river conditions. The representative values of QS and $S\sqrt{Q}$ for each reach are applied to the corresponding subreaches. As a result, all of the subreaches within a particular reach have the same values for QS and $S\sqrt{Q}$ over a given time period.

3.2.3. Sediment

Estimates of the median bed material size from samples at cross-sections are applied to the subreaches then time averaged for each time. Reach-averaged data are obtained using a weighted average of the subreach (Richard, 2001).

Another measure of flow energy proposed by Bledsoe and Watson (2001) combines driving (water discharge and channel slope) and resisting (bed material size) forces and is termed a "mobility index":

$$\mathrm{MI} = S\sqrt{\frac{Q}{D_{50}}} \quad (3)$$

with discharge in m^3/s and median grain size, D_{50}, in meters, the resulting units are $m/s^{0.5}$. The mobility index can also be thought of as a ratio of flow energy or unit stream power to the resisting force of the channel bed represented by the bed material grain size. Thus, it becomes an index of the erosive power of the flow or mobility capacity of the channel. A mobility index is computed for each reach and subreach for each time period using the peak daily discharge for the time period, the time-averaged slope, and the time-averaged bed material size.

Sediment supply for each reach is measured by the average suspended sediment concentration. A measure of bed material transport would be most appropriate to include, but these data are not available for the entire period of record. Prior to construction of Cochiti Dam, the flows in the Rio Grande were very turbulent. As a result, Woodson and Martin (1962) suggested that suspended sediment samples from the Rio Grande are more nearly indicative of the total load than similar samples from other rivers.

Average suspended sediment concentrations measured from double mass curves of cumulative annual water discharge and suspended sediment yield (Richard, 2001) are used. The reach-averaged values are applied to the appropriate subreaches as the suspended sediment concentration probably does not change between subreaches.

3.2.4. Channel width

Two different measures of channel width are measured at each cross-section line: the active channel width (W) and the total channel width (W_{tot}). The active channel width is the non-vegetated portion of the channel and does not include mid-channel bars or islands. The total channel width includes mid-channel bars and islands. For a single thread channel, the active channel width and the total channel width are identical. The subreach-averaged and reach-averaged values (Richard, 2001) of W and W_{tot} at the beginning of each time period are considered.

3.2.5. Planform

Four measures of channel pattern (Richard, 2001) are considered:

1. sinuosity, P=thalweg length/valley length;

Table 3
Independent variables used in regression models

Model no.	Independent variable
1	Q=Channel-forming discharge (m^3/s)
2	S=Slope at the beginning of the time period
3	QS=total stream power (m^3/s)
4	$S(Q)^{0.5}$=specific stream power $(m^3/s)^{0.5}$
5	MI=$S(Q/D_{50})^{0.5}$=mobility index $(m/s^{0.5})$
6	D_{50}=average median grain size of bed material (m)
7	W_{act}=active channel width at beginning of time period (m)
8	W_{tot}=total channel width at the beginning of the time period (m)
9	W_r=width ratio, W_{act}/W_{tot}
10	P=sinuosity at beginning of time period
11	P_{tot}=total sinuosity at beginning of time period
12	b=reach-averaged number of channels at beginning of time period
13	C=average suspended sediment concentration (mg/L)

2. total sinuosity, P_{tot}=total centerline channel length/valley length;
3. average number of channels, b; and
4. width ratio, W_r=active channel width/total channel width. The width ratio approaches a value of one as the channel moves toward single thread.

Values of each of the planform variables are measured from each digitized aerial photo of the active channel. The subreach and reach values of these parameters at the beginning of each time period are applied to the subsequent time period.

3.3. Statistical analysis

To determine the nature and amount of correlation between migration rate, M, and the independent variables, scatter plots are created and a correlation model is applied to log-transformed data. Application of the Pearson product moment correlation model indicates the nature (i.e., positive or negative) and degree of linear correlation between two variables. The resulting correlation coefficient, r, is 1 or −1 for perfect correlation and zero for no correlation (Pedhazur, 1997). The significance of each correlation is tested using an F-statistic and a corresponding p-value indicating the confidence level. All statistical analyses are performed using the SAS software package (SAS Institute, 2001).

An underlying assumption of the linear correlation model is that all of the samples are independent. Sampling different points along a river at different time periods could violate the presumption of independence. The result is that the p-value is artificially smaller than it should be and as a result is used with caution.

Scatter plots are created for each of the independent variables that demonstrated high correlation with migration rate. Different symbols are given to the pre-dam and post-dam reach-averaged data to visually demonstrate potential dam impacts. The subreach-averaged data are also plotted to illustrate the variability within the reaches.

3.4. Multiple regression analysis

Multiple regression analysis provides a useful tool for identification of significant relationships (Rhoads, 1992). The relationships that result from multiple regression analyses are an accessory to hypothesis, experience and intuition, but not a substitute for them (Chorley, 1966). We recognize the value of statistical analysis in identification of significant associations and also note that association does not prove causation.

The model parameters described above are used in $\log_{10}$-transformed regressions. First, each inde-

Table 4
Correlation coefficients (r-value) between reach-averaged log-transformed lateral migration rate and independent variables using 1918–2001 $\log_{10}$-transformed data

Independent variable	r-value	p-value
MI	0.776	<0.0001
W_{tot}	0.737	<0.0001
Q	0.736	<0.0001
D_{50}	−0.728	<0.0001
QS	0.721	<0.0001
dam	−0.717	<0.0001
$SQ^{0.50}$	0.655	0.0002
W_{act}	0.641	0.0002
C	0.575	0.001
W_r	−0.541	0.003
P_{tot}	0.418	0.027
b	0.403	0.034
S	0.270	0.165
P	0.269	0.167
Reach	−0.164	0.403

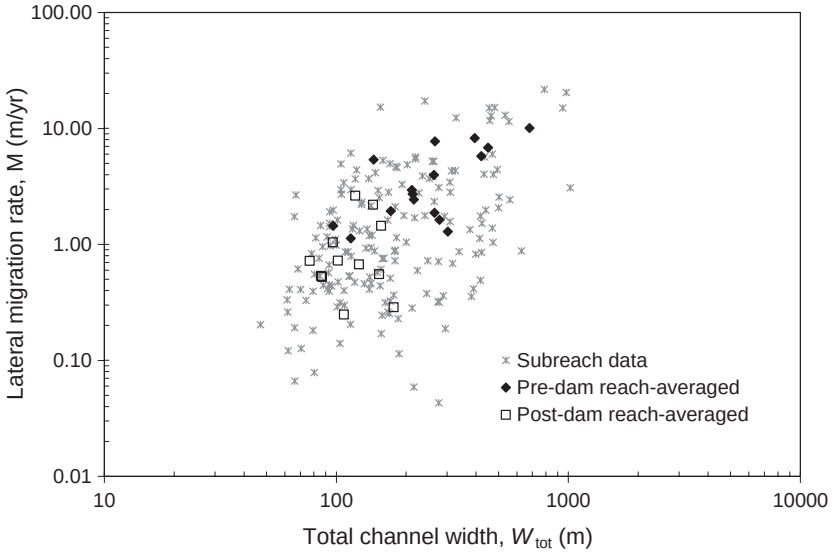

Fig. 2. Total channel width vs. lateral migration rate.

pendent variable individually (as shown in Table 3) is regressed against the lateral migration rate, M (Models 1–13). Multiple regression analyses with stepwise selection techniques ($\alpha = 0.05$) are then applied to different combinations of the measures of flow energy, width, and planform. The regression models are structured to compare the different measures of flow energy, width, and planform. Each measure of flow energy (Q, S, and D_{50} individually, $S\sqrt{Q}$, QS, and MI) is used in combination with each measure of width or width change (W_{act}, and W_{tot}) and of planform (P, P_{tot}, b, and W_r). The suspended sediment concentration is included in each model as an estimator of sediment supply. A total of 45 models are applied to the $\log_{10}$-transformed reach-averaged data and

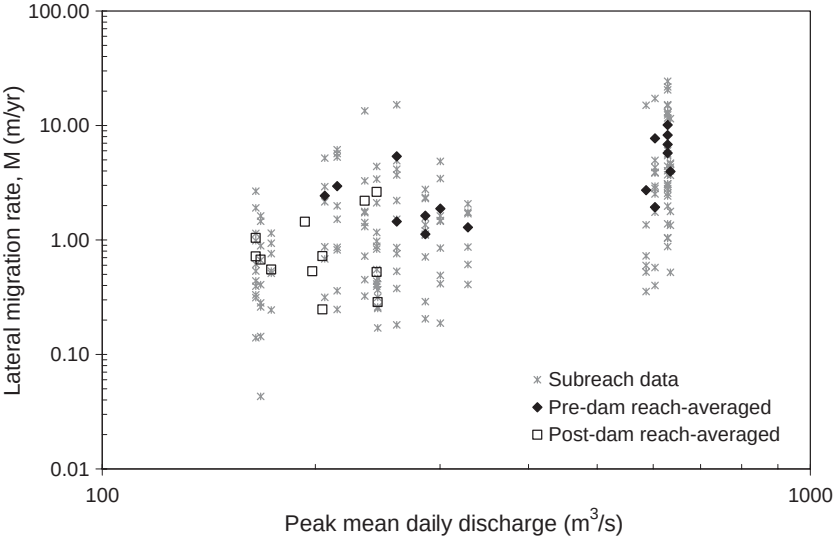

Fig. 3. Discharge vs. lateral migration rate.

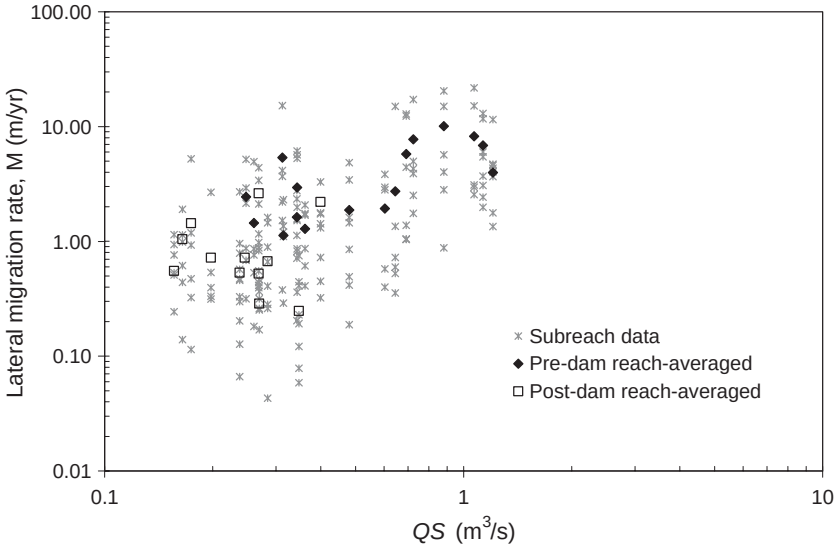

Fig. 4. Total stream power vs. lateral migration rate. *QS* vs. lateral migration rate.

the $\log_{10}$-transformed subreach-averaged data. The models utilize data from each time period from 1918–1992 using migration rate, *M*, as the dependent variable. Validation using the 1992–2001 data is performed using the equations with R^2-values> 0.50. The predicted migration rate is then compared with the observed and the percentage error calculated.

4. Results

4.1. Statistical analysis

Both the scatter plots and linear correlation models demonstrate associations between lateral migration rates and some independent variables. The linear correlations revealed significant ($p<0.01$, $r>0.5$)

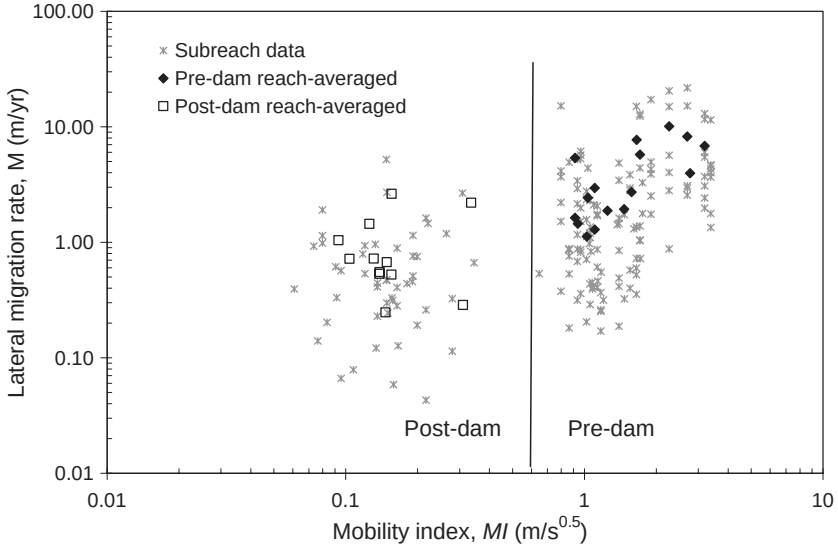

Fig. 5. Mobility index vs. lateral migration rate.

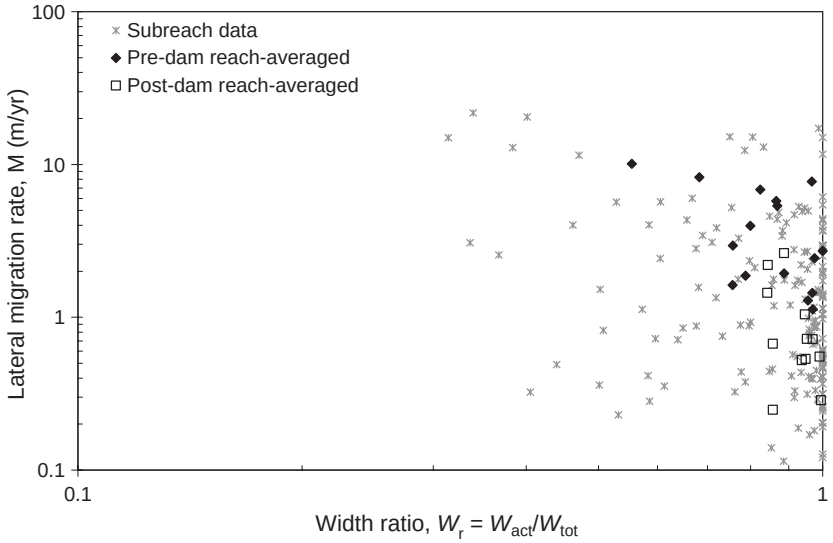

Fig. 6. Width ratio vs. lateral migration rate.

associations between migration rates and discharge, stream power, mobility index, width ratio, and channel width (Table 4).

The results in Fig. 2 clearly show: (1) separation between pre-and post-dam data; and (2) a trend toward increasing lateral migration with increasing total channel width. The trend in the subreach data is not so clear, and the scatter is much greater. The discharge vs. migration rate plot (Fig. 3) shows that the highest migration rates occur at the highest discharges for the pre-dam reach-averaged data. Similar patterns are evident in the total stream power (Fig. 4) and the mobility index plots (Fig. 5). However, the mobility index (Fig. 5) shows a clearer demarcation between the pre-and post-dam periods because the bed material size is in the denominator of the mobility index. Following construction of Cochiti Dam, the bed material size increased from sand to gravel size (Richard, 2001) resulting in a decline in the mobility index. Migration rates > 3 m/years do not occur at MI < 0.8. The measure of planform that produced the highest correlation with migration rate was the width ratio, W_r, (Fig. 6), which is the ratio of active channel to total channel width.

4.2. Multiple regression analysis

The equations resulting from the multiple regression analysis using reach-averaged data produced

Table 5
Results from the multiple regression analysis showing flow energy and planform variables best predicting reach-averaged migration rates (1918–1992) along the Cochiti section of the Rio Grande

$\log_{10}$-transformed regressions							
Dependent variable	Coefficient	Independent variable	Exponent	Partial R^2	p	Model R^2	p
M	1.83	MI	0.520	0.56	0.0004	0.61	0.0001
		W_r	−2.138	0.08	0.0433		
	0.0024	Q	1.120	0.53	0.0006	0.59	<0.0001
		W_r	−2.390	0.10	0.0251		<0.0001
	9.2	time period	−0.186		<0.0001	0.58	<0.0001
	6.3	QS	1.230		<0.0001	0.57	<0.0001
	2.6	MI	0.637		<0.0001	0.54	<0.0001
	2780	$SQ^{0.5}$	1.902		<0.0001	0.52	<0.0001
	0.0007	Q	1.380		<0.0001	0.51	<0.0001

higher explained variance ($R^2>0.5$) values than the subreach-averaged data ($R^2<0.4$). Results of the regression analyses that resulted in more than 50% explained variance are presented in Table 5. The decreased accuracy using the subreach data is likely a result of the natural variability in the system that is not accounted for by the chosen variables. For instance, bank material and stability, bank vegetation, variations in water slope with stage, and other details of cross-section and planform geometry are not included in these models although they may contribute to the local variability in the lateral migration rates.

The lateral migration rates for each time period (1918–2001) and each reach are computed using the equations resulting from the multiple regression analysis. The results producing the highest explained variance for each reach are plotted in Fig. 7. The accuracy of the "best" models ranges from 0.4 for reach 2 to 0.93 for reach 3, which is the least sinuous and the narrowest of the four reaches. The parameters that emerged as most significant in association with migration rates were flow energy (MI, Q, or QS) either alone or combined with a planform index (W_r).

Application of the six most accurate models to predict the 1992–2001 migration rates for each of the four reaches resulted in errors ranging from 1% to almost 600% (Table 6). Measurement of lateral channel variables at the subreach level do not increase the accuracy of the lateral movement predictions.

5. Discussion

5.1. Importance of channel planform

Other studies have shown relationships between lateral movement and channel width (Hooke, 1979; Brice, 1982; MacDonald, 1991). Brice (1982) noted that a line with a slope of 0.01 on a width vs. migration plot separates stable from unstable rivers and corre-

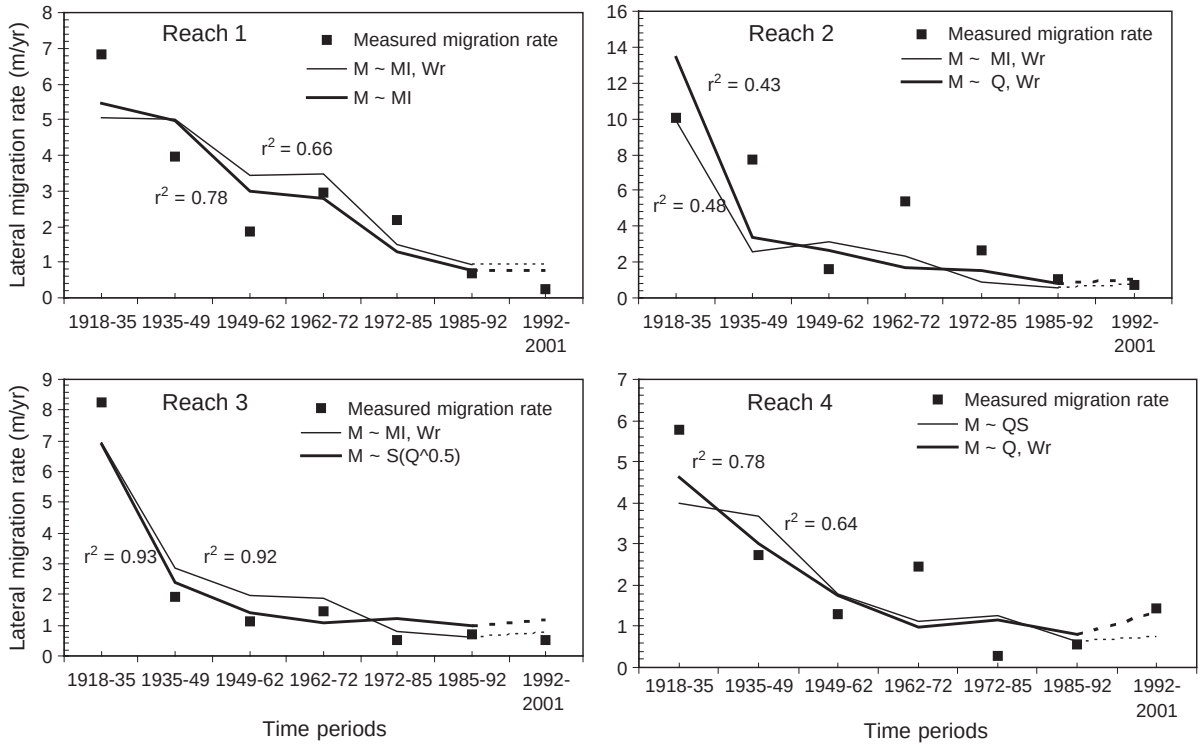

Fig. 7. Migration rates computed from the $\log_{10}$-transformed regression equations (Table 5) applied to the reaches 1 through 4 of the Cochiti section. The solid line represents calibration with 1918–1992 data, and the dashed line represents the validation with 1992–2001 data. The r^2-values are computed for 1918–2001.

Table 6
Validation of migration rate models using the 1992–2001 lateral migration rate results

$\log_{10}$-transformed regressions models	Reach no.	Observed 1992–2001 migration rate, M_{obs} (m/year)	Predicted 1992–2001 migration rate, M_{pred} (m/year)	Error $(M_{pred}-M_{obs})/M_{obs}$ (%)
$M=2.6\ MI^{0.637}$	1	0.25	0.77	209
	2	0.72	0.71	−1
	3	0.53	0.74	38
	4	1.44	0.69	−52
$M=1.83\ MI^{0.520}W_r^{-2.138}$	1	0.25	0.94	279
	2	0.72	0.71	−2
	3	0.53	0.73	37
	4	1.44	0.90	−38
$M=0.00071Q^{1.38}$	1	0.25	1.08	337
	2	0.72	1.08	50
	3	0.53	1.03	94
	4	1.44	1.00	−31
$M=0.0024Q^{1.12}W_r^{-2.39}$	1	0.25	1.34	442
	2	0.72	1.05	45
	3	0.53	1.02	91
	4	1.44	1.31	−9

sponds to migration rates that are 1% of channel width. Brice (1982) demonstrated that the line representing $M=0.01W$ also divided most equiwidth channels from most wide-bend and braided point-bar channels. All but two of the Cochiti section pre-dam reach-averaged migration rates plot above the $M=0.01W$ line (Fig. 8), indicating that these reaches could be classified as unstable. Most of the post-dam points fall below the $M=0.01W$ line, confirming the post-dam stable state identified by Richard (2001). The regression analyses revealed associations between planform variables and lateral migration rates. To compare the Cochiti section with other rivers, published lateral movement data compiled by Richard (2001) were plotted against channel width, along with the Cochiti section pre- and post-dam data (Fig. 9). The data were grouped by channel pattern in an attempt to see where the Cochiti section data and other published data fall within Brice's

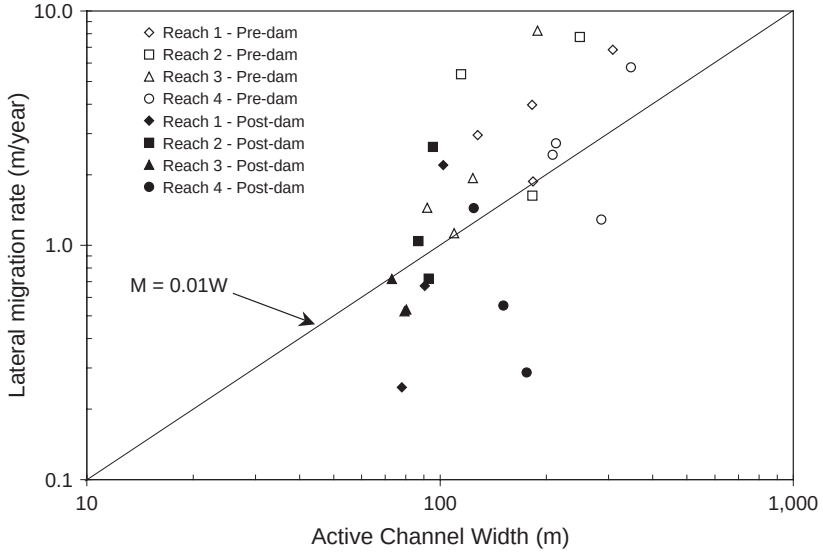

Fig. 8. Plots of active channel width vs. migration rate for reach-averaged data.

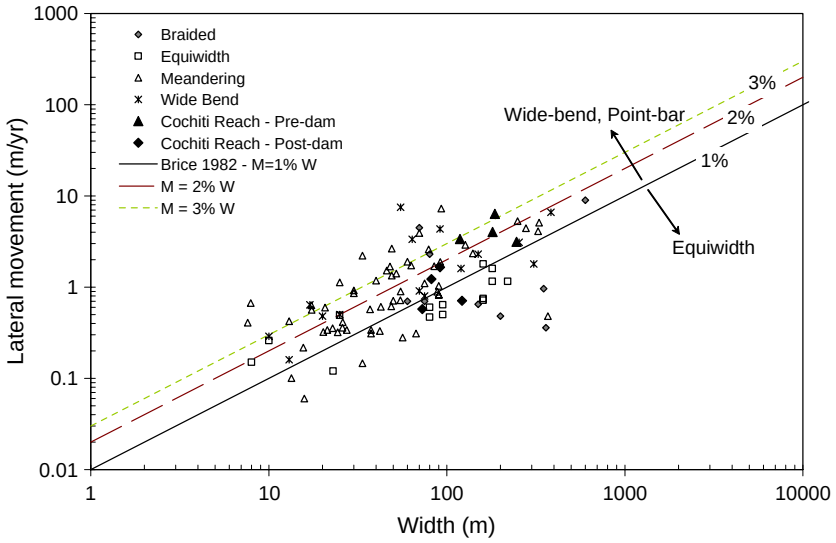

Fig. 9. Lateral movement rates vs. channel widths from Brice (1982), Hooke (1980), Klimek and Trafas (1972), MacDonald (1991), Nanson and Hickin (1986), and Shields et al. (2000) grouped by stream type compared with Cochiti section (Reaches 1–4) pre (1918–1972) and post-dam data (1973–2001).

(1982) channel type classification and with respect to the $M=0.01W$ line.

In order to compare the Cochiti section with the planform classification proposed by Brice (1982) and Chang (1985) based on downstream variability in width, the difference between widths of each subsequent cross-section was measured on the Cochiti section. The values were then reach-averaged and compared with the lateral migration rates for each reach and time period in Fig. 10. The downstream variability in width explains more than 50% of the variation in lateral migration rates ($p<0.0001$), with migration rates increasing with greater variability in width. The pre-dam channel exhibited greater variability in width and was more mobile than the post-dam channel.

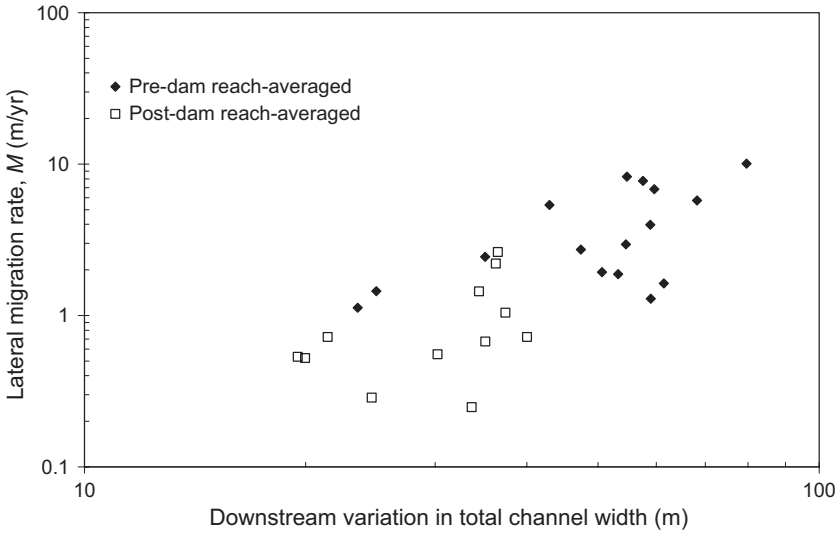

Fig. 10. Correlation of downstream variability in width and lateral migration rates for the Cochiti section (1918–2001).

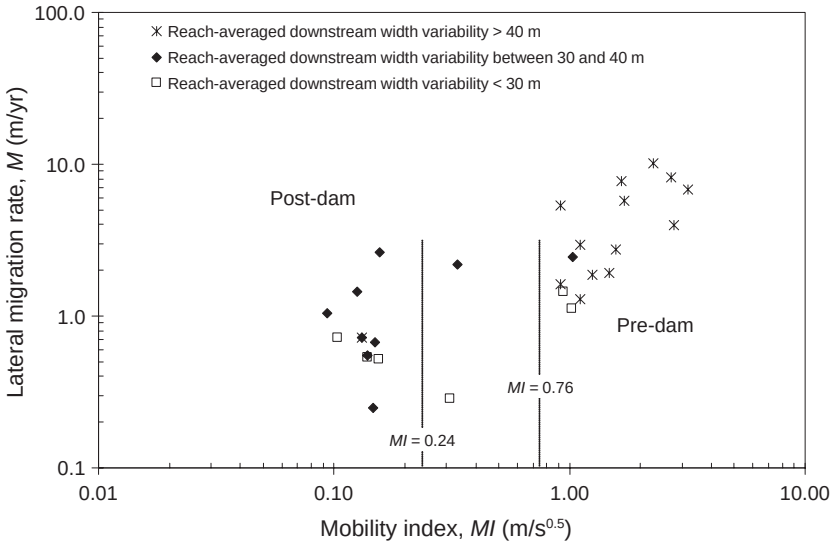

Fig. 11. Reach-averaged Cochiti section data (1918–2001).

Bledsoe (1999) determined that Chang's (1985) threshold from steep braided to braided and wide-bend point bar occurs at MI ≈ 0.76 m/s$^{0.5}$ and that the transition from braided and wide-bend point bar to straight braided occurs at MI ≈ 0.24 m/s$^{0.5}$. These thresholds are shown on Fig. 11, which shows the variability in channel width on a plot of lateral migration rates and mobility index for the reach-averaged Cochiti section data for 1918–2001.

5.2. Comparison of multiple regression models with other rivers

The equations resulting form the multiple regression analysis identify potentially important associations even though they do not explain more than 70% of the variance (Table 5). The variables that contributed most to the variability in migration rate are flow energy and planform. Studies by Nanson and Hickin (1986) and MacDonald (1991) resulted in equations to model lateral movement rates that can be compared with the results of this study (Table 7). The percent of explained variance (R^2-value) found in the models in this study are comparable to those found by Nanson and Hickin (1986). The highest values are <70%. Nanson and Hickin (1986) found that the highest explained variance (69.1%) was produced by a combination of Q, S, and D_{50} to model the variation in volume of migration measured by M^*h where h=bank height.

Table 7
Comparison of regression results with those from other studies

This study	Nanson and Hickin (1986)	MacDonald (1991)
$M=2.703Q^{1.2575}S^{1.1281}$ $R^2=0.55$	$M=1.663Q^{0.482}S^{0.368}$ $R^2=0.53$	
$M=208W_{act}^{0.0607}S^{1.47073}$ $R^2=0.37$	$M=0.301W^{0.895}S^{0.271}$ $R^2=0.54$	
$M=0.858W_{tot}^{1.0953}S^{0.7180}$ $R^2=0.47$		
$M=2780\left(S\sqrt{Q}\right)^{1.902}$ $R^2=0.52$	$M\cdot h=0.45\omega^{0.401}$ $R^2=0.20$	
$M=103\left(S\sqrt{Q}\right)^{1.378}D_{50}^{-0.190}$ $R^2=0.59$	$M\cdot h=0.607\omega^{0.823}D_{50}^{-0.207}$ $R^2=0.29$	
$M=0.004W_{tot}^{1.189}$ $R^2=0.47$		$M=0.28W^{0.0.34}$ $R^2=0.34$
$M=0.0007Q^{1.38}$ $R^2=0.51$		$M=0.022Q^{0.52}$ $R^2=0.75$

Difficulties arise in comparing the results of the equations from this study with those of others when variables are used in different forms. For instance, Nanson and Hickin (1986) used specific stream power, $\omega = \gamma \frac{QS}{W}$, while a surrogate for ω was used in this study, $S\sqrt{Q}$.

5.3. Spatial variability

In general, the results using the reach-averaged data perform better, indicating that there is more variability at the subreach level that is not accounted for in the parameters used in these models. Decreasing the spatial scale of measurement was anticipated to increase the accuracy of the regressions; however, this was not the case, which illustrates that there are other factors not accounted for in this study that contribute to the spatial variability in M in the Cochiti section. Such factors may include bank stability, vegetation, detailed cross-section geometry, meander geometry and randomness. Variation in bank material, stability, and height could play a significant role in both the temporal and spatial variability of migration rates along the reach.

5.4. Dam impacts

The bed material size, mobility index, and suspended sediment concentration were all highly correlated ($p<0.001$, $r>0.75$) with the presence of the dam. As shown by Richard (2001), the bed material coarsened and suspended sediment concentration decreased immediately following construction of the dam. Bed material size is in the denominator of the mobility index, so it decreases as bed material size increases. Discharge, stream power and channel width also correlate significantly with the presence of the dam ($p<0.005$, $r>0.5$). The declines in discharge and channel width were more gradual with time through the whole time period (Richard, 2001).

6. Conclusions

The 45-km Cochiti section of the Rio Grande, NM, provides an excellent case study in lateral response of an alluvial river to natural and anthropogenic alterations in water and sediment inflows. An extensive database that documents the changing water and sediment regimes and the corresponding lateral and vertical adjustments of the channel from 1918 to 2001 is utilized to quantify historic trends, measure indices of lateral mobility and stability, and model lateral movement rates.

Multiple regression models show that lateral migration rates are significantly associated with measures of flow energy and the ratio of active channel width to total channel width. Rates of change in active channel width were associated with the active channel widths at the beginning of the time period. The models explained up to 70% of the variability in migration rates for the 1918–1992 time period. The high degree of variability in the subreach-averaged data suggests that further detailed study of the bank composition, stability and cohesion, and vegetation at a smaller spatial scale could account for the unexplained variance in the subreach-averaged models.

The models are validated using the 1992–2001 lateral migration rate measurements from the Cochiti section. The regression equations using the mobility index or mobility index combined with width ratio predict the 1992–2001 migration rate with 75–89% average error. While the predictive capabilities of the models are obviously limited, they do highlight some significant associations between lateral mobility and flow energy and channel planform proposed by other studies. The construction of the Cochiti dam resulted in greater stability, shifting the channel toward a more stable, equiwidth configuration. The pre-dam planform geometry with higher rates of lateral migration demonstrates higher downstream width variability, and the post-dam channel demonstrates less variability in width and lower migration rates.

Acknowledgements

Funding from the U.S. Bureau of Reclamation (USBR) Albuquerque Office is gratefully acknowledged. However, the results do not necessarily reflect policies or endorsement of the USBR. Deepest thanks are extended to C. Leon and T. Bauer for their work

on development of the database. The authors are grateful to Paula Makar, Jan Oliver, and Viola Sanchez at the USBR.

References

Bauer, T.R., 1999. Morphology of the Middle Rio Grande from Bernalillo Bridge to the San Acacia Diversion Dam, New Mexico. MS Thesis, Colo. State Univ., Fort Collins, CO.

Begin, Z.B., 1981. Stream curvature and bank erosion: a model based on the momentum equation. Journal of Geology 89, 497–804.

Biedenharn, D.S., Combs, P.G., Hill, G.J., Pinkard Jr., C.F., Pinkston, C.B., 1989. Relationship between channel migration and radius of curvature on the Red River. In: Wang, S.S.Y. (Ed.), Sediment Transport Modeling. ASCE, NY, pp. 536–541.

Bledsoe, B.P., 1999. Specific Stream Power as an Indicator of Channel Pattern, Stability, and Response to Urbanization. PhD Dissertation, Colo. State Univ., Fort Collins, CO.

Bledsoe, B.P., Watson, C.C., 2001. Logistic analysis of channel pattern thresholds: meandering, braiding, and incising. Geomorphology 38, 281–300.

Brice, J.C., 1982. Stream Channel Stability Assessment, January 1982, Final Report. U.S. Deartment of Transportation, Federal Highway Administration, Washington, DC.

Bullard, K.L., Lane, W.L., 1993. Middle Rio Grande Peak Flow Frequency Study. U.S. Department of Interior, Bureau of Reclamation, Albuquerque, NM.

Carson, M.A., 1984. The meandering-braided river threshold: a reappraisal. Journal of Hydrology 73, 315–334.

Chang, H.H., 1985. River morphology and thresholds. Journal of Hydraulic Engineering 111, 503–519.

Chorley, R.J., 1966. The application of statistical methods to geomorphology. In: Dury, G.H. (Ed.), Essays in Geomorphology. American Elsevier Publishing Company, Inc., NY, pp. 275–387.

Dewey, J.D., Roybal, F.E., Funderburg, D.E., 1979. Hydrologic Data on Channel Adjustments 1970 to 1975, on the Rio Grande Downstream from Cochiti Dam, New Mexico Before and After Closure. U.S. Geological Survey Water Resources Investigations 79-70. U.S. Geological Survey, Albuquerque, NM.

Ferguson, R., 1987. Hydraulic and sedimentary controls of channel pattern. In: Richards, K. (Ed.), River Channels: Environment and Process. Basil Blackwell, Oxford, UK, pp. 129–158.

Hickin, E.J., Nanson, G.C., 1975. The character of channel migration of the Beatton River, northeast British Columbia, Canada. Bulletin of the Geological Society of America 86, 487–494.

Hickin, E.J., Nanson, G.C., 1984. Lateral migration rates of river bends. Journal of Hydraulic Engineering 110, 1557–1567.

Hooke, J.M., 1979. An analysis of the processes of river bank erosion. Journal of Hydrology 42, 39–62.

Hooke, J.M., 1980. Magnitude and distribution of rates of river bank erosion. Earth Surface Processes 5, 143–157.

Julien, P.Y., 2002. River Mechanics. Cambridge University Press. 434 pp.

Klaassen, G.J., Masselink, G., 1992. Planform changes of a braided river with fine sand as bed and bank material. In: Larsen, P., Eisenhauer, N.E. (Eds.), Sediment Management: 5th International Symposium on River Sedimentation. Karlsruhe, Germany, pp. 459–471.

Klimek, K., Trafas, K., 1972. Young-Holocene changes in the course of the Dunajec River in the Beskid Sadecki Mts. (western Carpathians). Studia Geomorphologica Carpatho-Balcanica VI, 85–91.

Knighton, D., 1998. Fluvial Forms and Processes—A New Perspective. John Wiley & Sons, Inc., New York.

Knighton, A.D., Nanson, G.C., 1993. Anastamosis and the continuum of channel pattern. Earth Surface Processes and Landforms 18, 613–625.

Lagasse, P.F., 1980. An Assessment of the Response of the Rio Grande to Dam Construction—Cochiti to Isleta Reach. U.S. Army Corps of Engineers, Albuquerque, NM.

Lagasse, P.F., 1981. Geomorphic response of the Rio Grande to dam construction. Environmental Geology and Hydrology in New Mexico, Special Publication-New Mexico Geological Society, vol. 10. New Mexico Geological Society, Albuquerque, NM.

Lagasse, P.F., 1994. Variable response of the Rio Grande to dam construction. In: Schumm, S.A., Winkley, B.R. (Eds.), The Variability of Large Alluvial Rivers. ASCE Press, New York, pp. 395–420.

Lawler, D.M., Grove, J.R., Couperthwaite, J.S., Leeks, G.J.L., 1999. Downstream change in river bank erosion rates in Swale–Ouse system, northern England. Hydrological Processes 13, 977–992.

Leon, C., 1998. Morphology of the Middle Rio Grande from Cochiti Dam to Bernalillo Bridge, New Mexico. M.S. Thesis, Colo, State Univ., Fort Collins, CO.

Leon, C., Richard, G., Bauer, T., Julien, P., 1999. Middle Rio Grande, Cochiti to Bernalillo Bridge, Hydraulic Geometry, Discharge and Sediment Data Base. Colorado State University, Fort Collins, CO.

MacDonald, T.E., 1991. Inventory and Analysis of Sstream Meander Problems in Minnesota. M.S. Thesis, Univ. of Minnesota, Minneapolis, MN.

Nanson, G.C., Croke, J.C., 1992. A genetic classification of floodplains. Geomorphology 4, 459–486.

Nanson, G.C., Hickin, E.J., 1983. Channel migration and incision on the Beatton River. Journal of Hydraulic Engineering 109, 327–337.

Nanson, G.C., Hickin, E.J., 1986. A statistical analysis of bank erosion and channel migration in western Canada. Geological Society of America Bulletin 97, 497–504.

Pedhazur, E.J., 1997. Multiple Regression in Behavioral Research. Holt, Rinehart and Winston, Inc., Fort Worth, TX.

Rhoads, B.L., 1992. Statistical models of fluvial systems. Geomorphology 5, 433–455.

Richard, G.A., 2001. Quantification and Prediction of Lateral Channel Adjustments Downstream from Cochiti Dam, Rio Grande, NM. PhD Dissertation, Colo. State Univ., Fort Collins, CO.

Richard, G.A., Julien, P.Y., 2003. Dam impacts on and restoration of an alluvial river-Rio Grande, New Mexico. International Journal of Sediment Research 18 (2), 89–96.

Sanchez, V., Baird, D., 1997. River channel changes downstream of Cochiti dam, middle Rio Grande, New Mexico. Proceedings of the Conference of Management of Landscapes Disturbed by Channel Incision. University of Mississippi, Oxford, MS.

SAS Institute, 2001. Statistical Analysis Software, The SAS System for Windows, ver. 8.02. The SAS Institute Inc., Cary, NC.

Schmidt, J.C., Everitt, B.L., Richard, G.A., 2003. Hydrology and geomorphology of the Rio Grande and implications for river rehabilitation. In: Garrett, G.P., Allan, N.L. (Eds.), Aquatic Fauna of the Northern Chihuahuan Desert. Museum of Texas Tech University, Lubbock, TX, pp. 25–45.

Shields Jr., F.D., Simon, A., Steffen, L.J., 2000. Reservoir effects on downstream river channel migration. Environmental Conservation 27, 54–66.

Thorne, C.R., 1991. Bank erosion and meander migration of the Red and Mississippi Rivers, USA. In: Van-de-Ven, F.H.M., Gutknecht, D., Loucks, D.P., Salewicz, K.A. (Eds.), Hydrology for the Water Management of Large River Basins (Proceedings of the Vienna Symposium, August 1991). International Association of Hydrological Sciences, pp. 301–313.

U.S. Army Corps of Engineers, 1978. Cochiti Lake, Rio Grande Basin, New Mexico, Water Control Manual. Appendix C to Rio Grande Basin Master Water Control Manual. U.S. Army Corps of Engineers, Albuquerque, NM.

U.S. Bureau of Reclamation, 1998. Rio Grande Geomorphology Study (1918–1992). USBR Remote Sensing and Geographic Information Group, Denver, CO.

Woodson, R.C., Martin, J.T., 1962. The Rio Grande comprehensive plan in New Mexico and its effects on the river regime through the middle valley. In: Carlson, E.J., Dodge, E.A. (Eds.), Control of Alluvial Rivers by Steel Jetties American Society of Civil Engineers ProceedingsWaterways and Harbors Division Journal, vol. 88. American Society of Civil Engineers, NY, pp. 53–81.

Xu, J., 1996. Underlying gravel layers in a large sand bed river and their influence on downstream-dam channel adjustment. Geomorphology 17, 351–359.

Xu, J., 1997. Evolution of mid-channel bars in a braided river and complex response to reservoir construction: an example from the Middle Hanjiang River, China. Earth Surface Processes and Landforms 22, 953–965.